Int. J. Electrochem. Sci., 13 **(2018)** 136 – 146, doi: 10.20964/2018.01.29

International Journal of
ELECTROCHEMICAL
SCIENCE
www.electrochemsci.org

Short Communication

Electrochemical Performance of Lead-Carbon Battery with Chitosan Composite Carbon / Lead Negative Plate

Hao Wang [1], *Zheng Liu*[1,*], *Haiying Li* [1], *Guo-Cheng Han* [2*], *Liang Yun* [1], *Hanyang Zhong* [1]

[1] College of Chemical And Biological Engineering，Guilin University of Technology，Guilin 541004, P.R. China
[2] School of Life and Environmental Sciences, Guilin University of Electronic Technology, Guilin, 541004, P.R. China
[*]E-mail: lisa4.6@163.com, hangc1981@163.com

Received: 10 September 2017 / *Accepted:* 30 October 2017 / *Online Published:* 1 December 2017

In this paper, chitosan carbon material with high specific capacity for the negative electrodes of lead-carbon battery was prepared by in-situ synthesis method. The chitosan carbon material was characterized by SEM (Scanning Electron microscope), EDS (Electron spectrum), BET and Raman spectrum. Electrochemical measurements were tested by electrochemical impedance spectroscopy (EIS) and cyclic voltammetry (CV). Moreover, the cycle life test and charge/discharge specific capacity curve were performed on battery performance testing system. It was turned out that the electrochemical performance of the negative plates made by chitosan was better with a larger specific capacitance, a smaller resistance plates and a longer discharge plateau compared with carbon black. The ultimate capacity of the cell was 108.72 mAh/g, the specific capacitance was 98% of the theoretical specific capacity after 10000 cycles. The cell performances test results showed that longer charge platform and higher ultimate capacity of chitosan composite carbon material modified lead-carbon battery.

Keywords: lead-carbon battery; negative material; in-situ synthesis; composite carbon material

1. INTRODUCTION

The car exhaust has become one of the main reasons resulting in the smog and the air pollution in city [1]. Therefore, energy conservation and emission reduction is a privileged direction on the automotive technology in the future [2]. In order to solve the two technical difficulties, the best way is vigorously developing the new energy vehicles, such as electric cars. In recent years, nation supported the development of electric vehicles and related industry strongly. The Ministry of Finance and other

four ministries issued jointly "the notice about the financial support on the new energy vehicles' popularization and application in 2016-2020" [3] which explicitly stipulated that the subsidies of the new energy automobile will be expanded to the whole country as well as the more rate of the decreasing later with the explanation that the subsidy in 2017-2018 will be eighty percent of the one in 2016 and the allowance in 2019-2020 will be 60% comparing with 2016 [4]. Thus, it is an urgently unresolved issues for all kinds of batteries that how to carry out the technical innovation and reduce the costs. The lead-carbon batteries will be the main force in the power market because of the advantages that low cost, facile industrial production and pollution-free production [5-7].

In lead-carbon batteries, conductive material was usually added in negative lead paste in order to build a conductive negative material. But the addition of the conductive material reduced the energy density to a certain extent. Therefore, it is significant to find a three-dimensional and high conductive material to construct an efficient conductive network. The energy density of the battery system can be improved by reducing the amount of the additives and raising the lead proportion of active material at the same time. The carbon material has the characteristics that excellent mechanical, electronic and heated conductive performance and controllable pore sizes [8-14]. After activating treatment, the material is widely used in energy storage due to its high specific surface area and fine electrical conductivity. Recent studies indicated lead-carbon batteries were substantially improved by the carbon addition in the negative plates [15-17] due to its high decentralization and conductivity. The addition of carbon materials [18-21] inhibiting the growth of $PbSO_4$ crystal in order to control the appearance of irreversible sulfate in lead-carbon batteries, and at the same time increased the utilization of active material in negative plates and reduce the lead usage amount effectively. Due to the existence of electric double layer structure, which improved the battery performance in the course of large current charging, lead-carbon batteries can be operated normally in the high rate charge and discharge process (HRPSoC) that the excellent capacitive characteristics of the carbon material can share a part of current under the condition of charging.

Since its wide range of raw material source and simple synthesis process, the biomass carbon material improving the utilization of natural resources and eliminate the pollution using the petrochemical resource to the environment caught the worldwide attention. Wang and coworkers [22] investigated that biomass derived carbon for energy storage devices drawing the conclusion on that various preparation methods have been developed for tailoring the properties of biomass derived carbon materials, including surface area, pore size distribution, surface chemistry and graphitization degree, etc. These properties mentioned above are relatively to the electrochemical performances of lead-carbon battery. Vasilescu and coworkers [23] reported the reactivity of Ti10Zr alloy in biological and electrochemical systems in the presence of chitosan indicating chitosan had a good electrochemical activity and bio-compatibility. And Saravanan and coworkers [21] reported that the negative additives of in-situ generated sugar derived carbon (SDC) improved the charging and discharging characteristics in the lead-acid batteries. In addition to providing a conductive network, SDC and lead oxide (LO) had a good effect on inhibiting the irreversible sulfate of the active substances. The specific storage of simulation battery which negative material was electrochemical carbon began to appear an obvious attenuation after the 30000 times in the high rate circulations, compared with the one of SDC which began to decay till the 50000 times. And the voltage of

simulation battery dropped more after 40 cycles appending the carbon-black. It can be seen that the SDC addition comparing with the traditional carbon additives, the utilization of active materials, cycling performance and charge acceptance had a significant improvement.

In this study, the composite carbon materials with high degree of graphitization, high specific surface area and high consistency were prepared by the chitosan and conductive agent (LO) with the method of in-suit synthesis. The electrochemical performance of in-situ generated chitosan composite carbon (SCC) and carbon-black composite material operating in lead-carbon battery was researched. The performances including specific capacity, cell impedance and charge/discharge cycle life were tested in order to evaluate the possibility of the negative materials in lead-carbon batteries.

2. EXPERIMENTAL

2.1 Preparation of composite carbon materials

Chitosan composite was prepared by the in situ synthesis method with two main steps [21].

Pretreatment: 2 g chitosan raw material (produced by China Sinopharm) was first immersed in 60 mL 2% acetum for 1 h, and then dried at 85℃ for 5h and grinded.

Synthesis Process: The sample prepared with the 76% degree of the LO was introduced into the muffle with a crucible carbonized at 800℃ under the nitrogen atmosphere with a heating rate of 5℃/min. The in-suit generated chitosan composite carbon material was gained after stabilizing at 800℃ for 2h and cooling to room temperature.

In addition, the carbon-black composite material was prepared by the same way as mentioned above.

2.2 Preparation of testing samples

In order to test electrochemical properties, lead paste (contents: 8.3 g chitosan composite carbon material, 50 g lead powder, 10 g $BaSO_4$, 0.5 g acetylene black, 0.5 g In_2O_3, 0.5 g Ga_2O_3, 20 mL PTFE emulsion and a little double-distilled water) mechanically agitating for 6h till the cream material generated was smeared uniformly on the plates and then dried at 65℃ for 8 h and subsequently stabilized at 75℃ for 6 h.

In order to perform battery tests, the simulated lead-carbon battery was assembled in a beaker with 1.28g/cm^3 H_2SO_4 solution. The plates placed on both sides separated by an industrial AGM partition was contacted to the Xinwei battery testing system in order to get the qualified positive and negative plates after formation. All positive and negative grids had a size of 4.0 cm × 7.0 cm (height × width) and thickness of 0.20 cm. The positive grids were produced by Baoji Changli Special Metal Co., Ltd and the negative grids were produced by Baoding Meilun Nonferrous Metal Co., Ltd.

2.3 Characterization Instruments

The X-ray powder diffraction pattern of the samples were characterized on a Holland Panalytical equipped with Cu K_α radiation source (λ = 1.54426 Å) under the current of 40 mA and the

voltage of 40 kV at the scanning rate of 16 °·min^{-1} in the range of 10 to 90°. The scanning electron microscopy pictures were taken on a Japan High-Techmpany Company S-4800 instrument under the voltage of 3 kV and the current of 10100 nA with the working distance of 6000 μm. Porous structure of the material was performed by nitrogen adsorption/desorption isotherms on the surface area analyzer produced in America Mike Instrument Company. Raman spectrum was tested on a confocal laser scanning microscope (America Thermo Company) observing that the peak intensity of D and G band.

The electrochemical performance testing was carried out by a common three-electrode system with self-made lead-carbon working electrode, standard calomel reference electrode and platinum auxiliary electrode in the H_2SO_4 electrolyte on a CHI860D workstation (Shanghai Huachen). The cyclic voltammogram test was performed in the potential window ranging from -1.20 to 0.80 V at different scanning rates(0.01 mV/s, 0.05 mV/s, 0.1 mV/s) vs. Hg/Hg_2SO_4 in 1.28 g/mL H_2SO_4 solution. The electrochemical impedance spectroscopy (EIS) was recorded by applying in a frequency range of 10^{-2} to 10^5 Hz with a AC amplitude of 5 mV at the room temperature. And the working performance testing of the battery was evaluated by using a Xinwei BTS high-precision battery testing system with the charge and discharge current of 0.12 A and 0.17 A, respectively.

3. RESULTS AND DISCUSSION

3.1 XRD and Raman spectra analysis

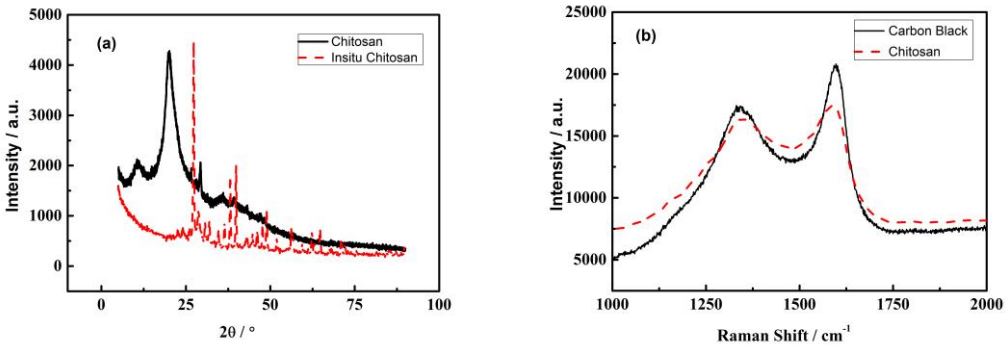

Figure 1. XRD spectra of chitosan and its composite carbon material (a) and Raman spectra of the composite carbon materials (b)

The XRD and Raman spectra of carbon composite material prepared by chitosan or carbon-black were shown in Fig.1 respectively. As shown in Fig.1 (a), the graphite diffraction peak, which was a broad peak, was observed at around 26.6° indicating that the structure of chitosan activated carbon was amorphous with a lower degree of graphitization. Fig.1 (b) displayed that the D peak appeared at 1340 cm^{-1} of both carbon-black and chitosan composite carbon materials belonging to A_{1g} module resulted from the Raman activity at the crystallization border area in carbon materials with the contribution of crystal size effect. Besides, the G peak was noticed at 1590 cm^{-1} belonging to E_{2g}

module appeared in all carbon fiber spectrums, which was the evidence that the graphite structure of chitosan was formed [24,25]. It was calculated that the intensity ratio of D peak and G peak was 0.81 and 0.90 respectively which indicated the graphitization degree and the electrical activity of the in-suit synthesis composite carbon material was higher [26].

3.2 SEM and EDS analysis

The scanning electron microscope local figures of composite carbon material were shown in Fig.2(a,b). It was seen that the surface of carbon-black was smooth and no pores compared with the chitosan composite carbon material which surface was loose and porous with interstitial and superficial pores leading to a larger specific surface area. The electrical double-layer capacitor offered by high specific surface area materials weakened the damage to negative plate at the high power charge / discharge and pulse discharge progress. In addition, the good conductive network was built in electrode material benefiting the electrolyte ion's rapid transference under the condition of high power charge and discharge with the aim that let the proton participate the electrochemical reaction in electric double layer through the pores [27]. Hence, the chitosan composite carbon material was more suitable than carbon-black as the negative material.

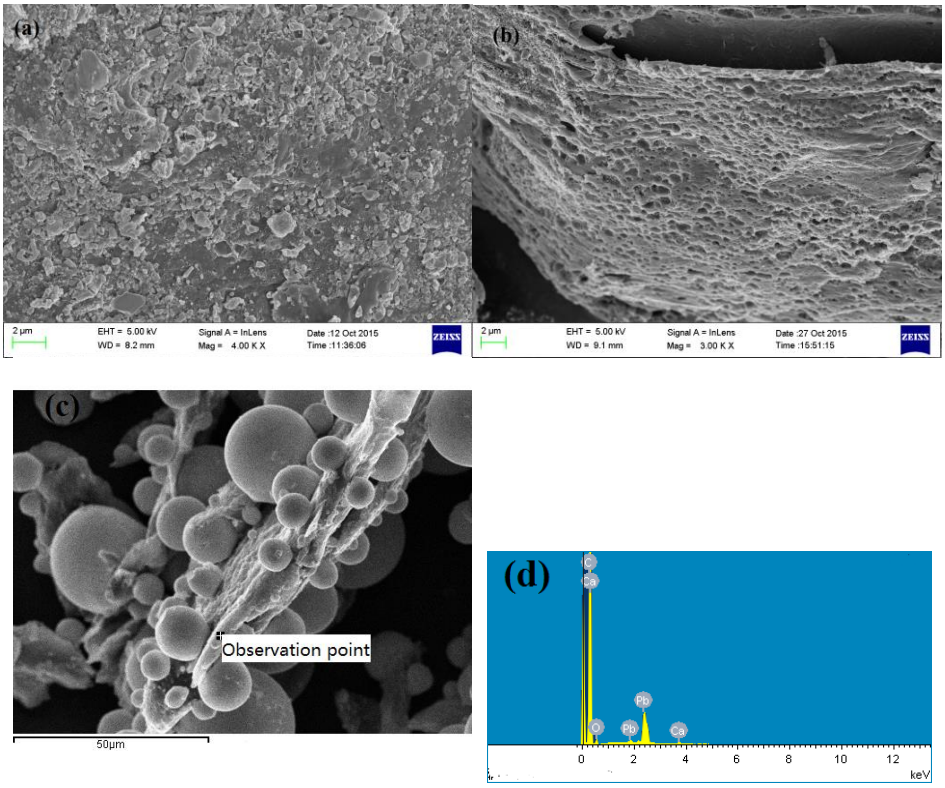

Figure 2. SEM image of chitosan composite carbon material (a,b) and EDS image of chitosan composite carbon material(c,d)

It was observed that the proportion of the carbon element was more than the lead in Fig.2(c,d) indicating the active material was distributed on the carbon plates. In other words, the electrochemical

performance was greatly promoted on account of the high-activity lead deposited on the surface of carbon material.

3.3 Specific surface area adsorption analysis

The nitrogen adsorption-desorption isotherms and pore size distribution curves for the composite carbon material were shown in Fig.3. According to the physical adsorption isotherm classification put forward by International Union of Pure and Applied Chemistry (IUPAC), the active carbon samples belonged to type IV isotherm [28]. At the low pressure area, the adsorption rate of the in-suit synthesis chitosan composite carbon material was rapider than the carbon-black indicating that chitosan composite carbon material contained a large number of pores. As the increase of the relative pressure, adsorption increment added slowly until forming a platform nearly parallel to the horizontal line. It was observed that the adsorption hysteresis loop at the relative pressure of 0.4 to 0.9 result from the mesopore in the material.

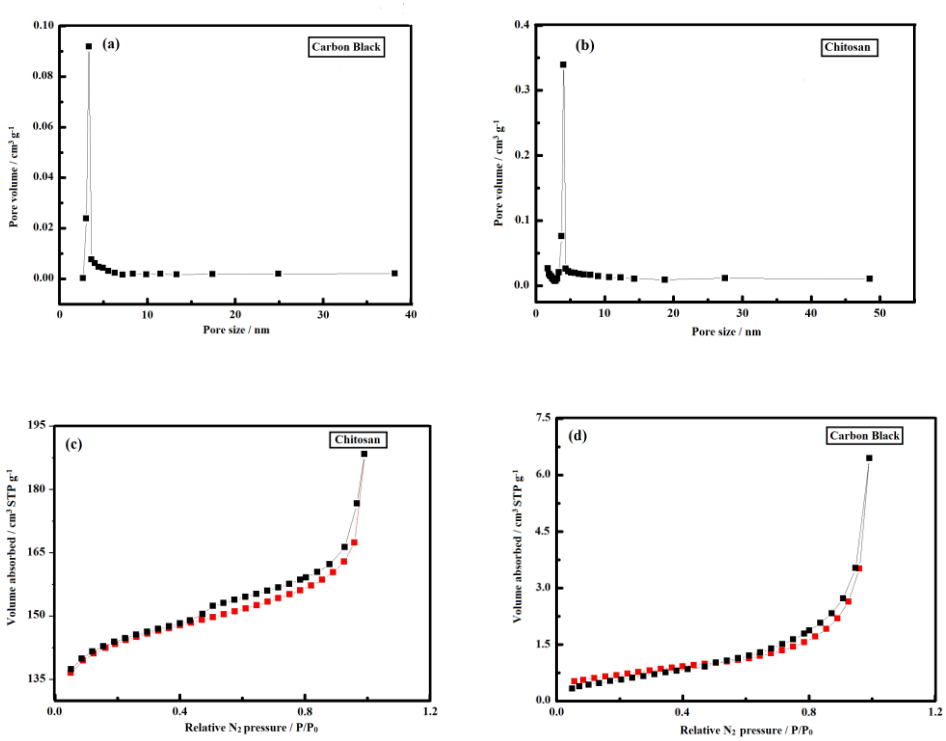

Figure 3. Particle size distribution of chitosan composite carbon material and carbon-black composite material

The pore sizes were distributed in 1 to 10 nm with the average size of 3.9 nm existing mesopore and micropore mainly. However, in the carbon-black composite material, the pore size mainly distributed in 3 to 20 nm with the mean pore size of 9.1 nm in main mesopore and macropore. As can be seen, carbon-black composite material exhibited a lower specific surface area of 5.561 m^2g^{-1}, and the chitosan composite carbon material presented a larger specific surface area of 487.4 m^2g^{-1}.

Due to the more micropore and mesopore and larger specific surface area in chitosan composite carbon material, the better conductive network was formed in order to enhance electronic transmission in negative plates [29]. The charge and discharge performance was improved by the capacitance characteristics, which could share a part of currents in charge process, in lead-acid battery. In conclusion, chitosan is a better carbon source to be chosen as negative composite material.

3.4 Electrochemical properties

3.4.1 Cyclic voltammograms

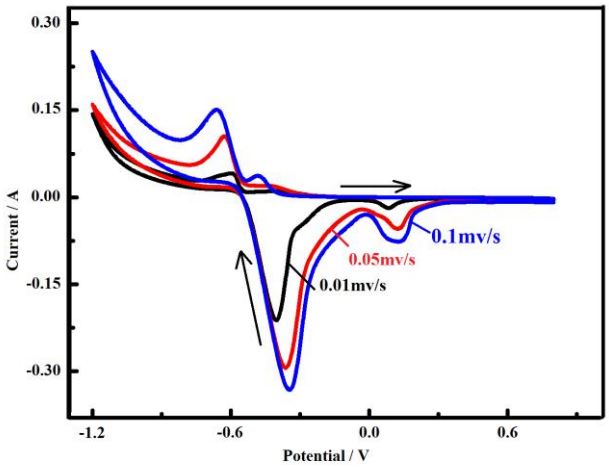

Figure 4. Cyclic voltammetry curves of chitosan composite carbon material at different scanning rates (The arrow shows the direction of scan)

It is seen in Fig.4 that two pairs of redox peak belonged to Pb/PbO_2, which the oxidation and reduction peak located at -0.8 V and -0.31 V, respectively, and H^+/H_2, which situated -0.7 V and 0.2 V severally comparing the above peak, has a obvious capacitance characteristics in the H_2SO_4 solution of 1.28 g/cm^3. Fig.4 shows the specific capacitance getting smaller as the increasing the scanning rate because that ions diffusion and electromigration has effect on the formation of the electrical double-layer capacitor [30]. The capacitor value is in relation to whether the ions have enough time to enter the micropore and interbedded pore in porous carbon microphores. According to the formula of $Cs=A/(2s\times\Delta V\times m)$, which s is the scanning rate, A is the rectangle area in cyclic voltammogram, ΔV is the range of the voltage and m is the mass of the active material, for the specific capacitance, the specific capacitance of in-suit composite carbon material is 162.9 F/g at the scanning rate of 0.1 mV/s.

3.4.2 Electrochemical impedance spectra

For a better apprehension of the electrochemical performance of the chitosan composite carbon/lead negative plate comparing with the carbon-black/lead negative plate, the electrochemical impedance spectra (EIS) was complied on the basis of the equivalent circuit [31] shown in Fig.5 (a).

Here, Rs and Rp were the negative material and electrolyte resistance respectively and CPE represents the capacitance in the interface between electrode and solution. Fig.5 (b,c) shows the EIS spectra of chitosan composite carbon/lead negative plate and the carbon-black/lead negative plate. Comparing with the two negative plates, it is concluded that the resistances are very different which the Rs value of 0.015892 Ω and 0.46525 Ω and the Rp of 1.872 Ω and 35.8 Ω. The changes of the resistance may be relative to the reason that capacitance, the constitution of the electrode and the electrolyte, the electrode placement and thinness. The most important factor is that the chitosan composite carbon materials have a good compatibility with the other additives in batteries. Moreover, a small charge transfer resistance is significant for negative plates to perform a favorable electrochemical performance [32,33].

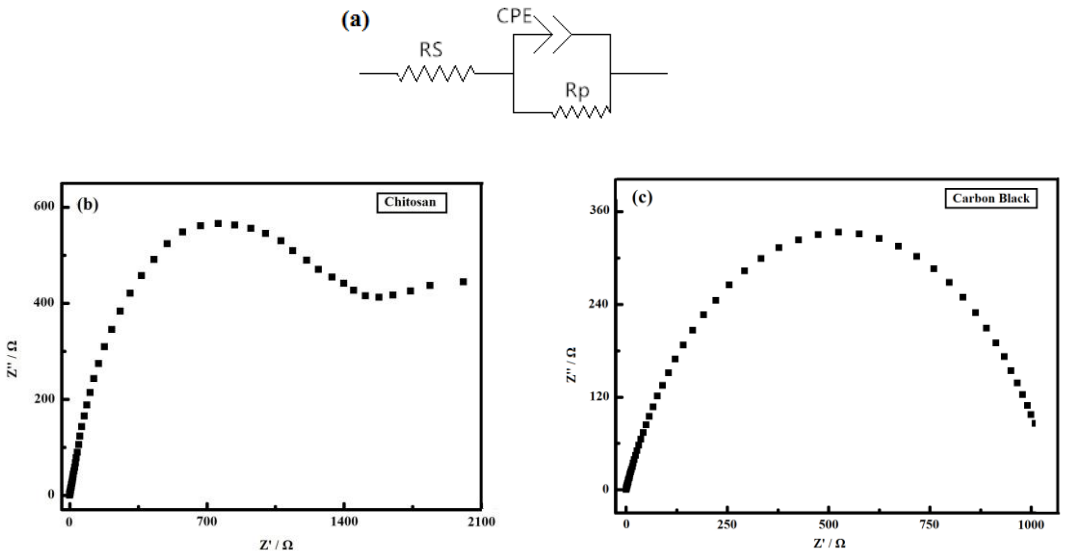

Figure 5. Analog circuit diagram(a) and EIS comparison plot (b, c) of composite carbon materials

3.5 Voltage specific capacity

The simulated cell assembled with lead paste mingling with the same proportion black-carbon and chitosan composite carbon material was measured by the first discharge curve test at the current of 750 mA on a full charge. It is seen easily in Fig.6 that the discharge voltage of the cell made of the chitosan composite carbon material is higher than the black-carbon and a longer discharge platform with an ultimate capacity of 108.72 mAh/g. Comparing to the carbon-black (86.13 mAh/g), the cell's capacitive property has raised 20.78%. A layer of carbon conductive network structure was formed on the surface of the active material compounded by chitosan benefitting the electron transfer and the penetration of the electrolyte and improving the utilization rate of the material by more decentralization. Besides, the electric double layer capacitor formed by the carbon material addition also improved the discharge performance of the cell.

Fig.7 shows the cycle life of lead-carbon battery in different carbon source additives under the condition of the same ratio. It is observed in the figure that the cell prepared with different carbon source additives is different in the percentage of theoretical specific capacitance after 10000 cycles, which the chitosan composite carbon material is 98% of the theoretical specific capacity, as well as having nearly no loss in capacity after 10000 cycles, and the carbon-black composite material is only 68%. Hence, according to the results, chitosan composite carbon material has a better efficiency and cyclic characteristics comparing with the carbon-black composite material. It is inferred that the conclusion above results from the secondary phase's formation surrounded by lead sulfate crystals limiting its growth space [34], which preventing the crystals from growing up in chitosan composite carbon materials. But the surface of negative active materials covered by lead sulfate along with the crystal's growth leading to stop the electrode reaction in black-carbon composite material. Besides, lead in negative plate maintains a higher activity due to the smaller lead sulfate crystals, which a plenty of crystals deposited on the surface of chitosan composite carbon material, at the time that the lead sulfate in negative plate translating into lead in the charging process. Because of the reasons above, the cyclic characterization of the cell has a significant improvement.

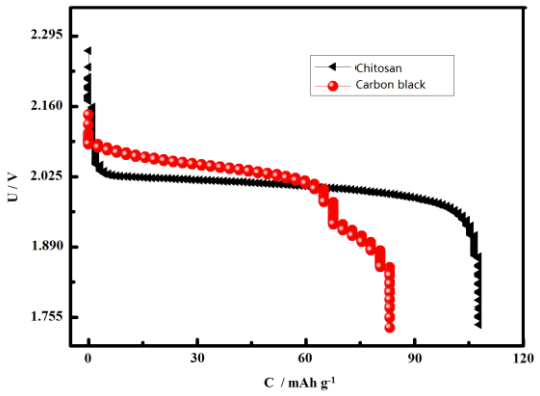

Figure 6. Initial discharge curves of different composite materials at 2C

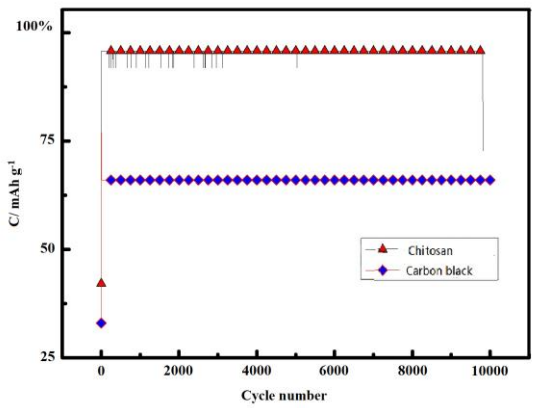

Figure 7. Cycle life curves of different composite materials

4. CONCLUSION

Chitosan composite carbon material was prepared with the simple method of in-situ synthesis from available biomass chitosan. According to SEM spectrum and BET result, it is concluded that the chitosan composite carbon material had a characteristics of an abundant and uniform honeycomb structure with a specific surface area of 487.4 m^2/g. And it is clear that the degree of graphitization is really suitable to use as electrode additives in the lead-carbon battery according to Raman spectrum. Through the method of electrochemical analysis, it is observed that a longer discharge platform of the cell prepared by chitosan with the ultimate capacity of 108.72 mAh/g paralleling with the carbon-black composite material tested by first charge and discharge analysis. The chitosan composite carbon material integrates to the negative activate mass and remarkably improves the electrochemical performance due to the low internal resistance. Therefore, the chitosan composite carbon material was synthesized can be used as a good additive in lead-carbon battery.

ACKNOWLEDGEMENTS
This work was supported by the National Nature Science Foundation of China (No. 21266006, 61661014, 61301038), the Nature Science Foundation of Guangxi Province (No. 2016GXNSFAA380109, 2015GXNSFBA139041) and Guangxi Key Laboratory of Electrochemical and Magneto-chemical Functional Materials, Collaborative Innovation Center for Exploration of Hidden Nonferrous Metal Deposits and Development of New Materials in Guangxi.

References

1. J. Wang, P. Nie, B. Ding, S.Y. Dong, X.D. Hao, H. Dou and X.G. Zhang. *J. Mater. Chem. A*, 5 (2017) 2411.
2. W.L. Zhang, J. Yin, Z.Q. Lin, J. Shi, C. Wang, D.B. Liu, Y. Wang, J.P. Bao and H.B. Lin . *J. Power Sources*, 342 (2017) 183.
3. X. Zhang and X. Bai. *Renew. Sust. Energ. Rev.*, 70 (2017) 24.
4. B.Q. Lin and R.P. Tan. *Energ. policy*, 104 (2017) 221.
5. D. Pavlov and P. Nikolov. *ECS Trans.*, 41 (2012) 71.
6. D. Pavlov and P. Nikolov. *J. Electrochem. Soc.*, 159 (2012) 1215.
7. B. Hong, L.X. Jiang, H.T. Xue, F.Y. Liu, M. Jia, J. Li and Y.X. Liu. *J. Power Sources*, 270 (2014) 332.
8. P. Křivík, K. Micka, P. Bača, K. Tonar and P. Tošer. *J. Power Sources*, 209 (2012) 15.
9. A. Banerjee, M.K. Ravikumar, A. Jalajakshi, P.S. Kumar, S.A. Gaffoor and A.K. Shukla. *J. Chem. Sci.*, 124 (2012) 747.
10. J. Furukawa, T. Takada, D. Monma and L.T. Lam. *J. Power Sources*, 195 (2010) 1241
11. X.P. Zou, Z.X. Kang, D. Shu, Y.Q. Liao, Y.B. Gong, C. He, J.N. Hao and Y.Y. Zhong.. *Electrochim. Acta*, 151 (2015) 89.
12. A.K. Shukla, A. Banerjee, M.K. Ravikumar and A. Jalajakshi. *Electrochimi. Acta*, 84 (2012) 165.
13. D. Pavlov, P. Nikolov and T. Rogachev. *J. Power Sources*, 196 (2011) 5155.
14. D.P. Boden, D.V. Loosemore, M.A. Spence and T.D. Wojcinski. *J. Power Sources*, 195 (2010) 4470.
15. M. Fernández, J. Valenciano, F. Trinidad and N. Muŕioz. *J. Power Sources*, 195 (2010) 4458.
16. K. Micka, M. Calábek, P. Bača, P. Křivák, R. Lábus and R. Bilko. *J. Power Sources*, 191 (2009) 154.

17. B. Rezaei, S. Mallakpour and M. Taki. *J. Power Sources*, 187 (2009) 605.
18. X.L. Li, Y.Y. Zhang, Z.L. Su, Y.J. Zhao, X.Y. Zhao and R.H. Wang. *J. Appl. Electrochem.*, 47 (2017) 619.
19. T. Sadhasivam, K. Dhanabalan, S.H. Roh, S.C. Kim, D. Jeon, J.E. Jin, J.Y. Shim and H.Y. Jung. *J. Mater. Sci.: Mater. Electron.*, 28 (2017) 5669.
20. A. Banerjee, B. Ziv, Y. Shilina, E. Levi, S. Luski and D. Aurbach. *ACS Appl. Mater. Interfaces*, 9 (2017) 3634.
21. M. Saravanan, M. Ganesan and S. Ambalavanan. *J. Power Sources*, 251 (2014) 20.
22. J. Wang, P. Nie, B. Ding, S.Y. Dong, X.D. Hao, H. Dou and X.G. Zhang. *J. Mater. Chem. A*, 5 (2017) 2411.
23. V.G. Vasilescu, I. Sandu, G. Nemtoi, A.V. Sandu, V. Popescu, V. Vasilache, G.S. Ioan and V. Elisabeta. *RSC Adv.*, 7 (2017) 13919.
24. E. Ebner, D. Burrow, J. Panke, A. Börger, A. Feldhoff, P. Atanassova, J. Valenciano, M. Wark and E. Rühl. *J. Power Sources*, 222 (2013) 554.
25. A. Sadezky, H. Muchenhuber, H. Grothe, R. Niessner and U. Pöschl. *Carbon*, 43 (2005) 1731.
26. T. Jawhari, A. Roid and J. Casado. *Carbon*, 33 (1995) 1561.
27. L. Wang, W.F. Zhang, L. Gu and H. Zhang. *Electrochim. Acta*, 222 (2016) 376.
28. G. Aranovich and M. Donohue. *J. Colloid. Interf. Sci.*, 200 (1998) 273.
29. W.J. Qian, J.X. Zhu,Y. Zhang and F. Yan . *Small*, 11 (2015) 4959.
30. C. Largeot, C. Portet, J. Chmiola, P.L. Tabema, Y. Gogotsi and P. Simon. *J. Am. Chem. Soc.*, 130 (2008) 2730.
31. A. Oury, A. Kirchev, Y. Bultel and E. Chainet. *Electrochim. Acta*, 71 (2012) 140.
32. I. Yang, S.G. Kim, S.H. Kwon, M.S. Kim and C.J. Ji. *Electrochim. Acta*, 223 (2017) 21.
33. B.L. Corso, I. Perez, T. Sheps, P.C. Sims, O.T. Gül and P.G. Collins. *Nano Lett.*, 14 (2014) 1329.
34. S. Rada, M.L. Unguresan, L. Bolundut, M. Rada, H. Vermesan, M. Pica and E. Culea. *J. Electroanal. Chem.*, 780(2016)187.